MDPI

Effect of Nanosized Precipitates on Corrosion Resistance of Nb-Microalloyed Steels

Irina Rodionova [1], Nataliya Arutyunyan [2,*], Andrey Amezhnov [1], Dmitrii D'yakonov [1], Yuliya Gladchenkova [2], Sergey Dunaev [2] and Irina Vasechkina [1,3]

[1] Bardin Central Research Institute of Ferrous Metallurgy, 105005 Moscow, Russia; igrodi@mail.ru (I.R.); amejnov@mail.ru (A.A.); aberkas@yandex.ru (D.D.); i.vasechkina@chermet.net (I.V.)
[2] Faculty of Chemistry, Lomonosov Moscow State University, 119991 Moscow, Russia; jubykova@yandex.ru (Y.G.); dunaev@general.chem.msu.ru (S.D.)
[3] Department of New Materials and Nanotechnologies, National University of Science and Technology MISIS, 119049 Moscow, Russia
* Correspondence: naarutyunyan@gmail.com; Tel.: +7-495-939-1673

Abstract: High-strength cold-rolled low-carbon microalloyed steels are widely used in the automotive industry. Preference is generally given to microalloying with niobium, since its effect on the mechanical properties of steel is most pronounced due to both precipitation hardening and a reduction in the ferrite grain size. For the operation of a car, the corrosion resistance of metal parts is an important factor, since, along with other properties of the material, it determines its service life. The study of the effect of the structural state of cold-rolled sheet low-carbon Nb-microalloyed steels, processed in continuous annealing units, on their corrosion resistance has been carried out. Methods of optical, scanning and transmission electron microscopy, mechanical and corrosion tests were used. It is shown that one of the main structural factors that determine the corrosion resistance of rolled products is the size of nanosized NbC precipitates. The influence of the temperature parameters of hot rolling and annealing on their formation has been established. An increase in the temperatures of the hot rolling end and coiling, as well as annealing, leads to an increase in their average size in the rolled stock after annealing, which increases the corrosion resistance of the steels under consideration.

Keywords: corrosion resistance; microalloyed steels; continuous annealing; cold-rolled steel; auto-sheet steels; nanosized precipitates; niobium carbide

1. Introduction

High-strength cold-rolled low-carbon microalloyed steels with a tensile strength of more than 400 MPa, subjected to processing in continuous annealing units (CAU), are widely used in the automotive industry. These steels have simultaneously high mechanical (strength, ductility, and formability), technological and service properties [1,2]. Due to low their carbon concentration, these steels have good weldability and corrosion resistance. The required level of strength is achieved mainly through grain refining and precipitation hardening. These two mechanisms of strengthening are controlled by the precipitation of excessive phases [1,3]. In this case, niobium carbonitride or carbide most effectively slow down the recrystallization of austenite, thereby contributing to a decrease in the grain size of ferrite [4,5]. This additionally increases strength and improves ductility and toughness [6]. Nanosized titanium and vanadium carbides, when precipitated during the $\gamma \to \alpha$ phase transformation, most effectively increase the strength of steel [7–9]. As recent studies show, a sharp increase in strength can be achieved when the size of precipitates is from 2 to 6 nm [6,10–13], which is consistent with the model [14]. Dispersed carbide precipitates can act as irreversible traps of hydrogen, and thus contribute to an increase in the resistance of steel against hydrogen embrittlement [3,15,16]. Moreover, the best trapping ability was achieved for carbides less than 3 nm in size [17,18]. Therefore, in recent

decades, active research has been carried out on the process of the formation of phase precipitates and the effect of their type, size, quantity and morphology on the mechanical and service properties of steel [13,19].

Despite the above-mentioned positive effects of dispersed phase precipitates on various properties of low-carbon steels, the results of recent studies have shown that the presence of nanosized carbide precipitates worsens the resistance of microalloyed steels against atmospheric corrosion [20] and under operating conditions of oil-field pipelines [21,22]. It was estimated that precipitates with a size of ~2–3 nm have the greatest effect [20–23].

It should be noted that these individual works do not yet allow us to make an unambiguous conclusion for the development of the most optimal technological modes of production. Therefore, to ensure a sufficient level of corrosion resistance for cold-rolled low-carbon microalloyed steels, a more complete base of information on the corresponding role of nanosized phase precipitates is required. This work aimed at solving this problem. Its goal was to determine the influence of the parameters of thermal deformation treatment of cold-rolled low-carbon Nb-microalloyed steels, processed in continuous annealing units, on the characteristics of nanosized precipitates of niobium carbide and, as a result, on the corrosion resistance of the cold-rolled products.

2. Materials and Methods

The study was carried out using samples of cold-rolled sheet products of a thickness of 1 mm of converter steels with the chemical composition shown in Table 1. The most significant feature of steel No. 2 is the higher content of manganese and niobium.

Table 1. Chemical composition of the investigated steels, wt.%.

Steel No.	C	Si	Mn	S	P	Cr	Ni	Cu	N	Al	Nb
1	0.06	0.03	0.47	0.009	0.01	0.03	0.03	0.06	0.006	0.034	0.026
2	0.07	0.07	0.73	0.007	0.01	0.04	0.03	0.06	0.006	0.043	0.050

Hot rolling of continuously cast slabs was carried out on a continuous broadband mill in three different modes. The main parameters of hot rolling (T_6—temperature of the end of rolling in the roughing group of stands; T_f—finishing temperature of rolling; T_c—temperature of coiling) are provided in Table 2.

Table 2. Parameters of hot rolling and processing of rolled products in CAU.

Steel No.	Batch No.	T_6, °C	T_f, °C	T_C, °C	Annealing Temperature, °C							
					P3	P4	P5	P6	P7	P10	P11	P12
1	1-1	1010	840	575	734	756	767	681	431	412	356	309
2	2-1	1052	856	585	732	756	764	678	430	411	355	311
2	2-2	1052	854	580	748	778	783	680	430	420	362	312

The strips obtained were subjected to cold rolling to the required thickness with the same degree of reduction, i.e., of 70%, heat treatment, and temper rolling at 1.2%. Heat treatment was carried out in a combined continuous unit designed for processing cold-rolled steel without coating (mode of continuous annealing unit—CAU), as well as for processing cold-rolled steel with the application of a zinc coating (mode of hot-dip galvanizing unit HG). The investigated rolled products were treated according to the CAU mode (Figure 1), in which the temperatures indicated as P2–P7 and P10–P12 were controlled. Temperatures P8 and P9 were controlled during the processing of rolled products according to the HG mode, therefore, they are not shown. The cooling rate during slow cooling was 2 °C/s, with accelerated cooling it was 30 °C/s.
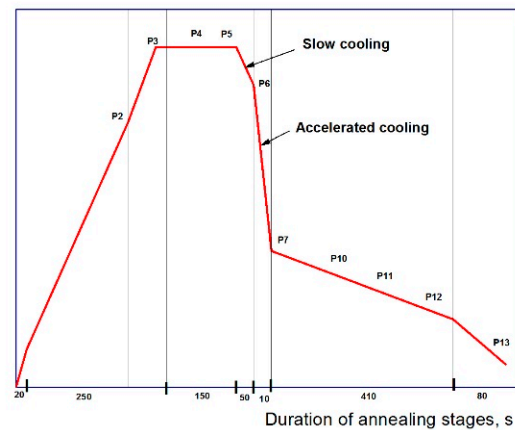
Figure 1. Scheme of heat treatment of cold-rolled steels in a continuous annealing unit (CAU): Pi—strip temperatures at the exit from the zones of heating sections (P2, P3), holding (P4, P5), slow cooling (P6), accelerated cooling (P7), overaging (P10, P11, P12) and final cooling (P13).

A metallographic examination was carried out using a NEOFOT optical microscope (Carl Zeiss, Oberkochen, Germany). For each steel, the secant method was used to determine the size of the ferrite grain along and across the rolling direction D_x and D_y, the average value of the size in two directions D_a, and the coefficient of grain elongation D_x/D_y. Using an HECKERT FP-100/1 tensile testing machine (VEB MWK Fritz Heckert, Chemnitz (Karl-Marx-Stadt), Germany (GDR)), the following mechanical properties were determined: tensile strength (σ_B), yield strength (σ_T), and relative elongation (δ).

Corrosion tests of samples of cold-rolled steel were carried out by means of the alternating immersion method, consisting of the cyclic immersion of metal samples in an 3.5% NaCl aqueous solution, holding for 10 min at a temperature of 22 °C and then drying in air for 50 min, followed by a determination of the change in the sample weight per unit area of the working surface. The method of the corrosion resistance evaluation was based on the standard of American Society for Testing and Materials (ASTM). However, in contrast to the ASTM standard, the corrosion resistance was assessed not by the weight loss of the samples, but by the specific weight gain (weight increase) of the samples during the test—[$\Delta m/S$], where Δm is the change in the sample weight during the test (g) and S is the corroded working area of the sample (m^2). This value characterizes the amount of corrosion products formed during the test. This technique is substantiated in detail in [24]. The corrosion process proceeds in two opposite directions within each cycle—loss of mass due to the anodic process of electrochemical corrosion; an increase in mass due to the formation of insoluble iron hydroxides (compounds of iron with oxygen and water, i.e., rust) and their adhesion to the surface of the sample. The process of removing corrosion products from the sample surface to determine its weight loss is less convenient, since if a strictly prescribed regime is not followed erroneous results can be obtained. Therefore, when comparing the corrosion resistance of steels of a similar composition, it is more convenient to use a characteristic such as weight gain. It is obvious that higher values of the specific weight gain correspond to a lower corrosion resistance of the steel. It has been empirically established that the most reliable and reproducible test results are obtained by measuring the weight gain of a metal sample after 30 immersion cycles [24]. This method has been successfully applied to study the corrosion resistance of a number of cold-rolled steels, including low-carbon microalloyed steels [20,24,25].

To determine the composition of nonmetallic inclusions, a JSM-6610LV (JEOL Ltd., Tokyo, Japan) scanning electron microscope (SEM) with an INCA Energy Feature XT attachment for an energy dispersive analysis was used. The microstructure was studied by transmission electron microscopy (TEM) on a JEOL device (JEOL Ltd., Tokyo, Japan) completed with an EM-ASID3D2 scanning attachment and a LINK SYSTEM SERIES II attachment for energy-dispersive X-ray microprobe analysis at 15,000–30,000 times the

working magnification, accelerating voltage of 120 kV and spatial resolution ≈ 1 nm. Samples for research were cut across the rolling direction.

The temperature of the onset of niobium carbide precipitation was determined using a thermodynamic computer model [26], implemented on the basis of proprietary software (Bardin TsNIIChermet, Moscow, Russia), by finding the conditions of thermodynamic equilibrium in multicomponent, multiphase systems at specified external and internal parameters (temperature, pressure, chemical composition). As a result, the types of equilibrium phases, their quantities and compositions were determined by an analysis of the complete possible set for the alloying system of steels under consideration.

3. Results

The results of mechanical and corrosion tests are shown in Table 3. It can be seen that the strength characteristics of rolled products No. 1-1 and corrosion resistance are lower than those of the rolled products No. 2-1 and 2-2. These differences are most likely due to the different content of manganese and niobium (Table 1) and, as a consequence, the difference in the dispersion and morphology of ferrite, as well as the presence of precipitates of niobium carbide.

Table 3. Results of mechanical and corrosion tests.

Steel No.	Batch No.	Mechanical Properties			Corrosion Rate
		σ_T, MPa	σ_B, MPa	δ, %	$\Delta m/S$, g/m^2
1	1-1	335	416	26.5	8.7
2	2-1	375	492	22.5	5.7
2	2-2	371	468	23	5.7

3.1. Investigation of Nonmetallic Inclusions

To exclude the factor of the influence of nonmetallic inclusions, which can provoke corrosion processes, on the corrosion resistance of investigated rolled products [27], an analysis of the contamination with nonmetallic inclusions was carried out.

For all steel samples, the results of optical microscopy showed the presence of point and line oxides (Figure 2a), as well as very thin extended sulfide lines (Figure 2b). The number and size of inclusions of all these types in the samples of the three rolled products under study are similar.
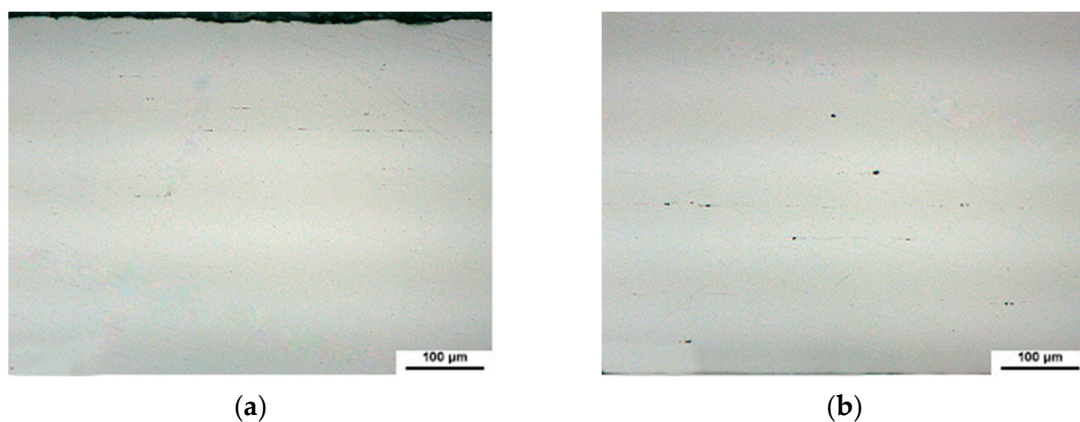

(**a**)   (**b**)

Figure 2. Nonmetallic inclusions in the samples of the batches: (**a**) Point and line inclusions (No. 2-2); (**b**) Extended inclusions (No. 2-1).

The results of the SEM study (Figure 3) showed that most of the nonmetallic inclusions present have a complex composition. The oxide component is corundum with a small

addition of magnesium, the sulfide component is manganese sulfide, sometimes with the addition of calcium. It is important that the composition of inclusions in samples of different rolled products has a similar composition
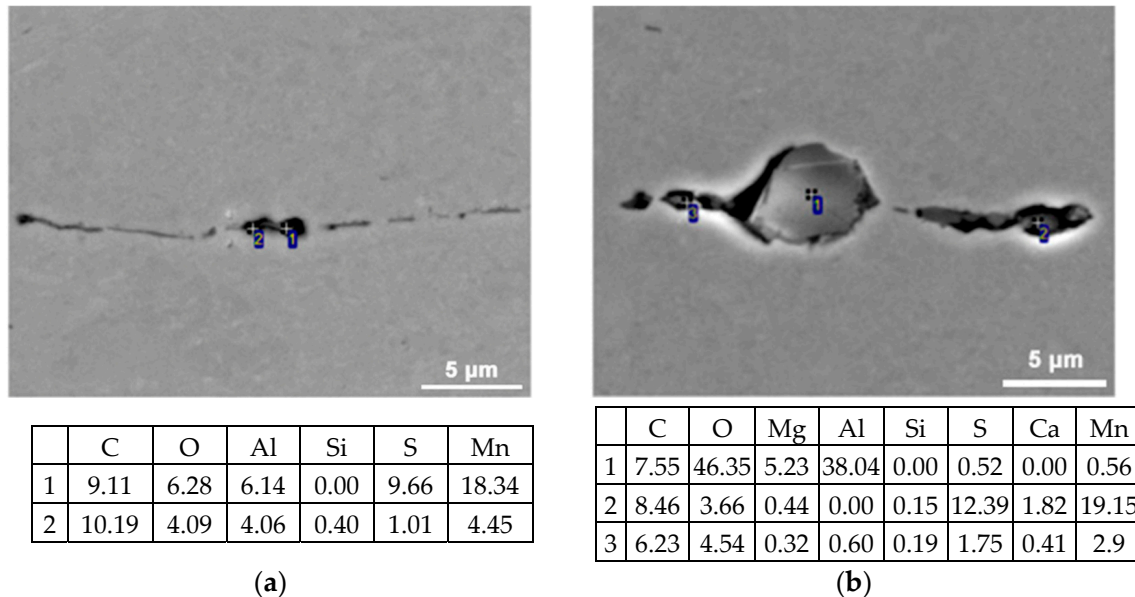

	C	O	Al	Si	S	Mn
1	9.11	6.28	6.14	0.00	9.66	18.34
2	10.19	4.09	4.06	0.40	1.01	4.45

(**a**)

	C	O	Mg	Al	Si	S	Ca	Mn
1	7.55	46.35	5.23	38.04	0.00	0.52	0.00	0.56
2	8.46	3.66	0.44	0.00	0.15	12.39	1.82	19.15
3	6.23	4.54	0.32	0.60	0.19	1.75	0.41	2.9

(**b**)

Figure 3. View and composition of inclusions in samples of the batches: (**a**) No. 1-1; (**b**) No. 2-2.

Thus, the number and composition of nonmetallic inclusions in the studied samples of all three rolled variants are close. Therefore, the factor of contamination with nonmetallic inclusions is not responsible for the different corrosion resistances of the steels under study.

3.2. Microstructure Investigation

The results of the microstructure study are shown in Figure 4. The microstructure is ferrite–pearlite. No noticeable difference in the grain size across the thickness of the samples was revealed. Table 4 shows the parameters of the grain microstructure of the studied samples. It can be seen that no significant differences in the grain size of samples of various rolled products were observed, but rolled products No. 2-1 and No. 2-2 present a slightly more dispersed microstructure.

Table 4. Grain size in the test samples.

Batch No.	D_y, μm	D_x, μm	D_x/D_y	D_a, μm
1-1	4.79	6.91	1.44	5.85
2-1	3.95	7.25	1.83	5.6
2-2	3.80	6.10	1.61	4.95

The structural characteristics of the samples were studied in more detail by TEM. The results showed that the matrix structure of all samples is identical. It is based on polygonal ferrite (Figure 5a). The density of dislocations in ferrite ranges from low to moderate. The carbon-rich regions are present in the form of degenerate pearlite. The size of such areas, as a rule, is several micrometers, rarely about 10 μm. Cementite is also found occasionally in the form of precipitates along the boundaries of ferrite grains and at their junctions (Figure 5b).
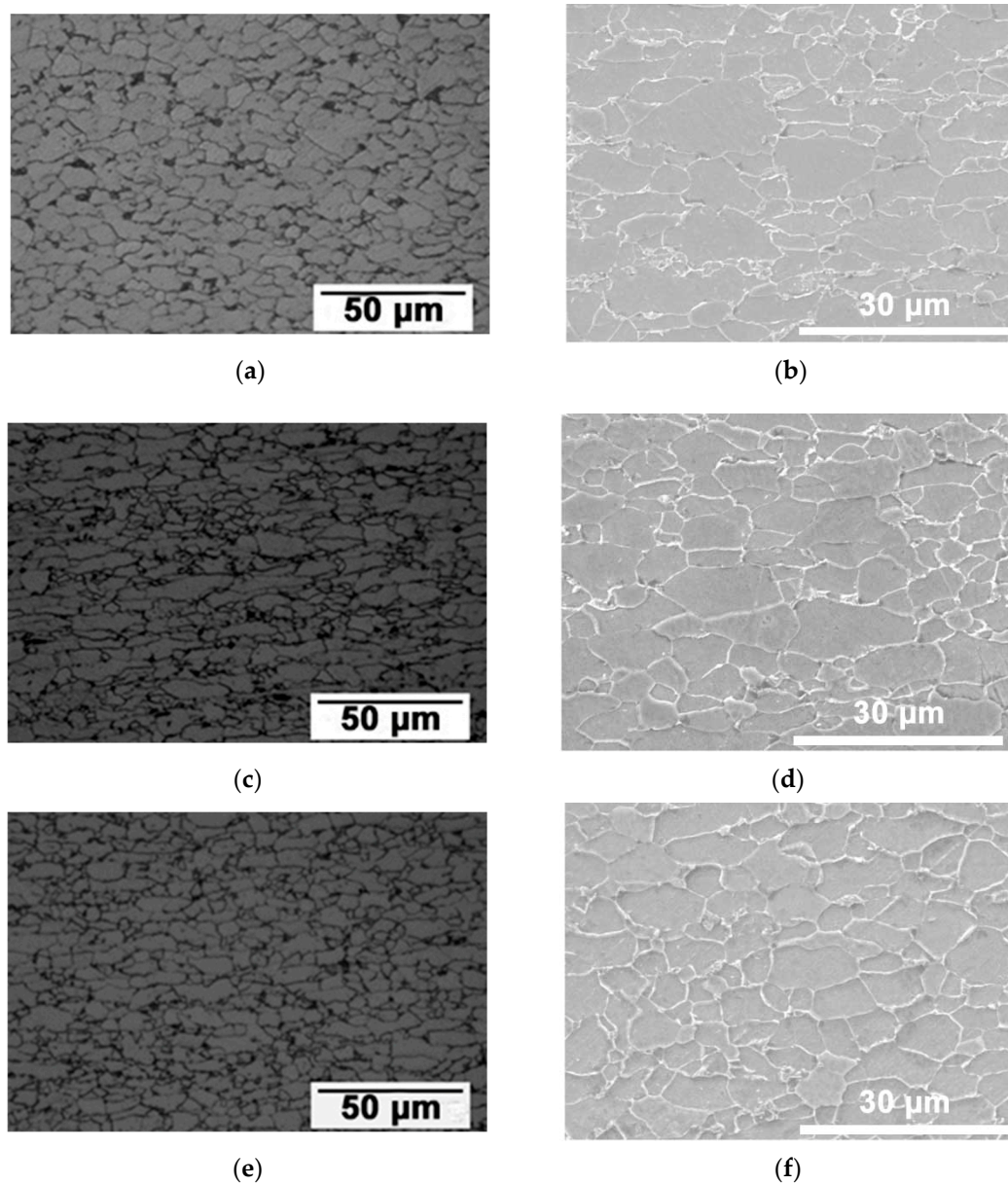
Figure 4. Microstructure of samples of the batches: (**a**,**b**) No. 1-1; (**c**,**d**) No. 2-1; (**e**,**f**) No. 2-2.
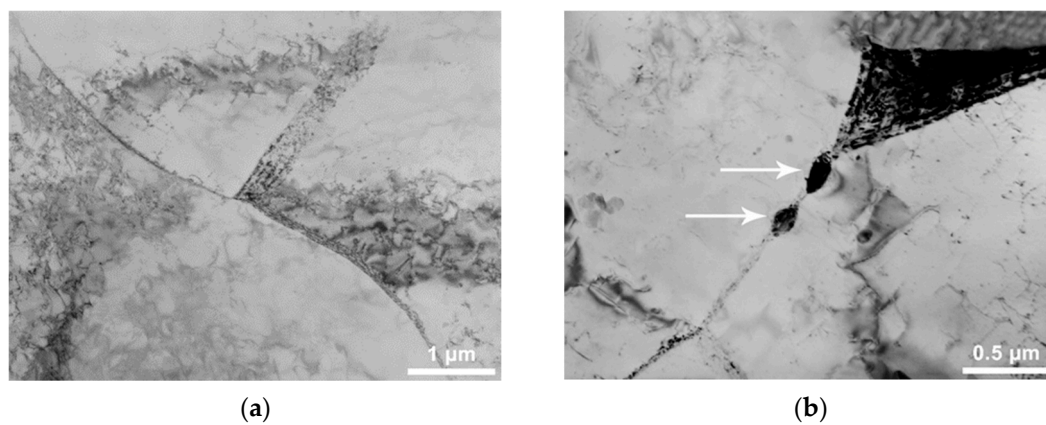

Figure 5. Microstructure of samples of the batches (TEM, bright-field images): (**a**) Polygonal ferrite (No. 1-1); (**b**) Cementite precipitation indicated by arrows (No. 2-2).

3.3. Investigation of the Precipitation of Excess Phases

In all samples of the investigated steels, precipitates of particles of various sizes were found. As a result of calculating the interplanar distances from the reflections of such particles in microdiffraction patterns, it was established that they belong to niobium carbide with an fcc lattice ($d_{200NbC} = 0.222$ nm, $d_{220NbC} = 0.157$ nm).

Submicron precipitates are practically absent in batch No. 1-1 (they are rare). Figure 6a shows the largest of these particles. Batches No. 2-1 and No. 2-2 contain many more submicron particles (Figure 6b). Their sizes are generally of up to 30–50 nm. There is also a small number of particles of 60–80 nm and a few of up to ~200 nm.
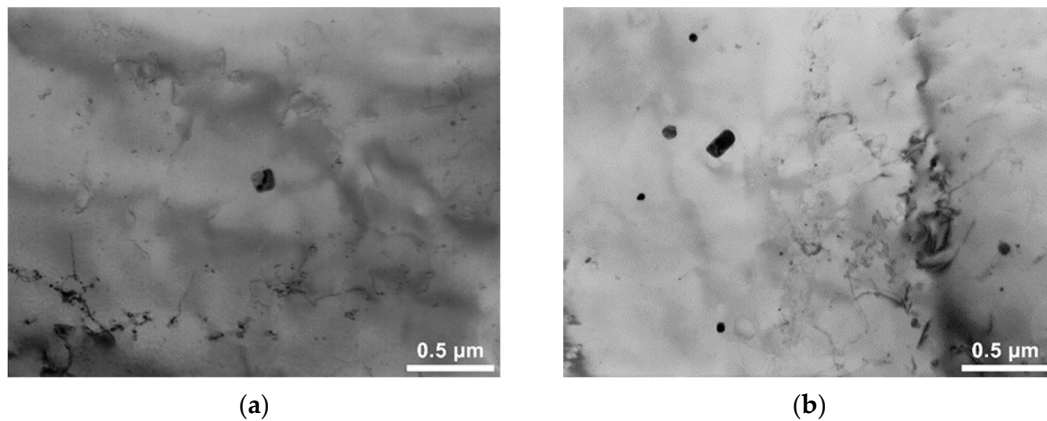

(a)	(b)

Figure 6. Submicron precipitates in samples of the batches (TEM, bright-field images): (**a**) No. 1-1; (**b**) No. 2-2.

Nanosized carbide precipitates can be found in any area of all the samples tested for their presence (Figure 7). The number of particles varies greatly from site to site. Sometimes areas with a bulk density of particles much higher than the average are found (Figure 7b). In general, in batches No. 2-1 and No. 2-2, the particles are larger than in No. 1-1, and their number is higher. The dominant size of precipitates in the batch No. 1-1 is 2–5 nm, some reach 6–8 nm and particles of up to 10–12 nm are rare. In samples of steel No. 2 with a higher niobium content, the precipitates are larger. In zones where they are relatively small, their size for batches No. 2-1 and No. 2-2 is 2–6 and 2–8 nm, respectively, in zones with relatively larger particles, the size of individual particles reaches 10–12 and 10–15 nm.
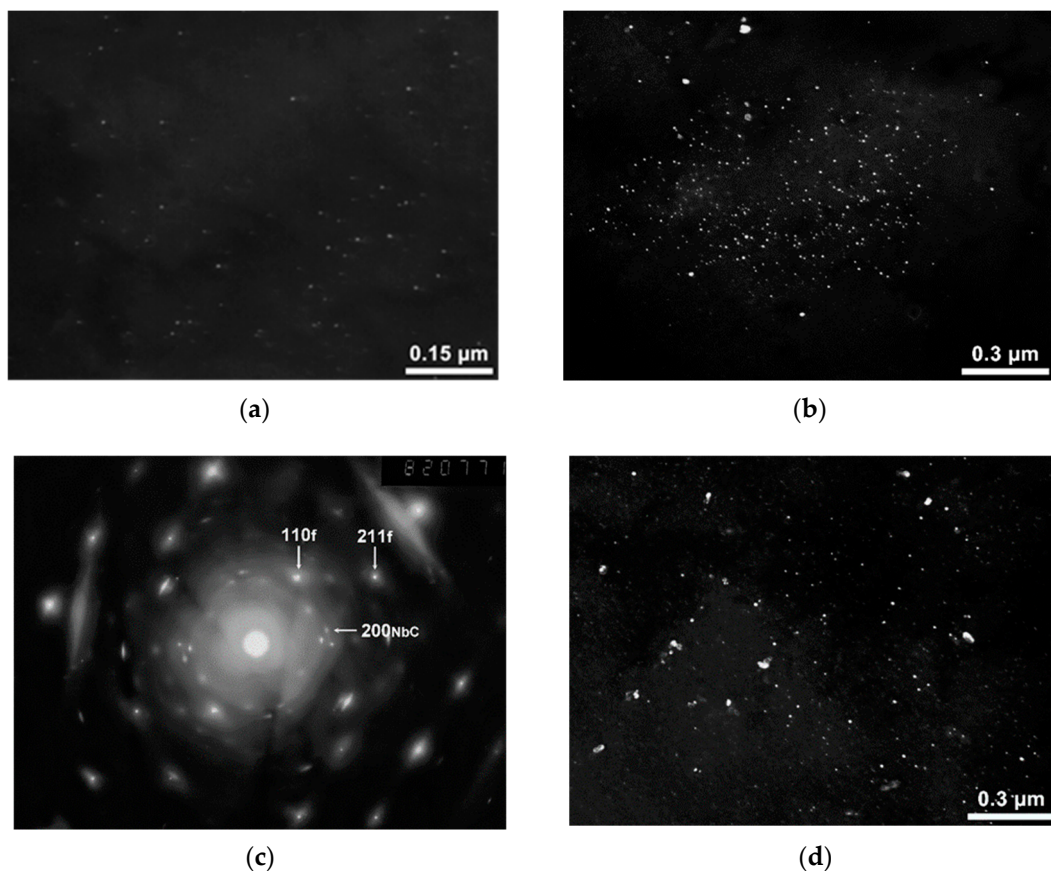
Figure 7. Nanosized NbC particles in samples of the batches (TEM): (**a**) No. 1-1; (**b**) No. 2-2; (**c**) No. 2-2; (**d**) No. 2-1. Dark-field images in reflections of nanocarbides (**a,b,d**) and microdiffraction pattern with marked reflections of NbC and (some) ferrite—f (**c**).

4. Discussion

The results of the study show that rolled steel No. 2 that contains 0.05 Nb has a higher corrosion resistance (Table 3). The main difference between the two chemical compositions is the manganese and niobium content. It was shown in [28] that manganese has little effect on the corrosion resistance of microalloyed steels. However, later, in [29], it was found that with an increase in the Mn content to 2.0 wt.% the corrosion resistance of low-alloy steels increases due to grain refinement and the formation of a protective rust layer. The higher corrosion resistance of steel No. 2 with increased manganese content is in good agreement with the results [29].

Moreover, one of the factors that determine the resistance of auto-sheet steels against atmospheric corrosion, which proceeds by an electrochemical mechanism, is the structural state of rolled products, including the dispersion of the microstructure, the density of dislocations, and the characteristics of precipitates of excessive phases [20].

As follows from Table 4, rolled products No. 2-1 and No. 2-2 have a slightly more dispersed microstructure. Therefore, due to the contribution of grain-boundary hardening, the strength of these samples is higher than that of rolled products No. 1-1. Apparently, the decrease in grain size is associated with a higher content of niobium and a higher temperature T_6 (1052 °C), which contributed to the deceleration of the recrystallization processes. This is due to both the precipitation of niobium carbide initiated by deformation and to the drag effect, i.e., a slowing down of the movement of grain boundaries by the dissolved niobium atoms on them [4]. This conclusion is confirmed by the presence of a greater number of submicron-sized precipitates in rolled products No. 2-1 and No. 2-2 and their absence in No. 1-1. According to [20,25], the formation of a larger amount of

submicron precipitates in hot rolled strip is caused by an increase in temperature T6, which correlates with the temperature of heating the slabs for rolling. An increase in the latter leads to a more complete dissolution of niobium when heated for rolling. In addition, an increase in the niobium content leads to an increase in the temperature range at the onset of niobium carbide precipitation. According to the thermodynamic calculation, the temperatures of the onset of NbC precipitation for compositions No. 1 and No. 2 are 1100 °C and 1168 °C, respectively. Thus, in rolled products No. 2-1 and No. 2-2, the precipitation of carbide particles begins earlier, thereby making it possible to form fine grains of austenite and, subsequently, fine grains of ferrite in hot rolled products.

As follows from [30–32], a more dispersed microstructure is one of the positive factors for improving corrosion resistance. This is due to an increase in the stability of the passive film, which is especially evident in materials with the finest grains. At the same time, a noticeable difference in corrosion resistance occurs when the grain size differs by several orders of magnitude [33,34]. Therefore, in the case of rolled products No. 2-1 and No. 2-2, this factor is not significant.

A comparison of the microstructure of the studied samples shows that in all samples the main structural component is polygonal ferrite and there are no noticeable differences in the dislocation structure. Therefore, this factor also does not affect the corrosion resistance in this case.

The most significant difference in the study of the structural state is observed in the presence of nanosized precipitates of niobium fcc-carbide. In rolled products No.1-1, particles with a smaller size dominate. A feature of the technology for producing hot rolled stock for samples of steel No. 2 was higher temperatures at the end of rolling. In this case, due to the greater supersaturation of the solid solution with carbon before coiling, most of the nanosized particles were formed during the cooling of the coiled coil. Therefore, the additional precipitation of niobium carbide during annealing occurred mainly due to their growth, which facilitated the formation of larger nanosized precipitates in the finished rolled products. In addition, at elevated annealing temperatures, a coagulation of nanosized precipitates of niobium carbide occurs. For samples of rolled products No. 1-1, the formation of a large number of isolated nanosized particles occurred in the process of annealing. At the same time, the annealing temperatures P3, P4, P5 for rolled products No. 1-1 were lower than for rolled products No. 2-2, therefore, their growth and coagulation occurred to a small extent. The annealing temperature of rolled products No. 2-1 was also lower. Therefore, even though size of precipitates in rolled products No. 2-1 is larger than in No. 1-1, most of the precipitates were smaller than in No. 2-2. This explains the higher strength of this rolled product (Table 3). Despite the higher annealing temperature used for rolled products No. 2-2, its structure is more dispersed than in the case of No. 2-1. This is seemingly due to both the finer grains before annealing and the inhibition of grain growth by the already existing nanosized particles. At the same time, due to the reduction in mechanical stresses resulting from cold deformation, the strength of rolled products No. 2-2 is slightly lower than No. 2-1. The size of nanosized precipitates for samples No. 2-2 is the largest and reaches 8 nm, and in zones with relatively larger particles, of15 nm.

Thus, the study carried out indicates that the most likely reason for the lower corrosion resistance of rolled products No. 1-1 is the small size of the niobium carbide precipitates. To increase the corrosion resistance, it is advisable to use, firstly, higher temperatures at the end of hot rolling (T_6, T_f) and coiling, so that the maximum amount of niobium carbide precipitates before annealing, and secondly, to use higher annealing temperatures to ensure the growth of nanosized particles and their coagulation.

Data Availability Statement: Not applicable.

Conflicts of Interest: The authors declare no conflict of interest.

References

1. Lesch, C.; Kwiaton, N.; Klose, F.B. Advanced high strength steels (AHSS) for automotive applications—Tailored properties by smart microstructural adjustments. *Steel Res. Int.* **2017**, *88*, 1700210. [CrossRef]
2. Pouraliakbar, H.; Khalaj, G.; Jandaghi, M.R.; Khalaj, M.J. Study on the correlation of toughness with chemical composition and tensile test results in microalloyed API pipeline steels. *J. Min. Metall. Sect. B-Metall.* **2015**, *51*, 173–178. Available online: http://www.jmmab.com/images/pdf/2015/23_soctwccttrmaps-nov-2015-173-178.pdf (accessed on 1 January 2022). [CrossRef]
3. Villalobos, J.C.; Del-Pozo, A.; Campillo, B.; Mayen, J.; Serna, S. Microalloyed Steels through History until 2018: Review of Chemical Composition, Processing and Hydrogen Service. *Metals* **2018**, *8*, 351. [CrossRef]
4. DeArdo, A.J. Niobium in modern steels. *Int. Mater. Rev.* **2003**, *48*, 371–402. [CrossRef]
5. Garcia, C.I.; Hua, M.; Cho, K.; DeArdo, A.J. On the strength of microalloyed steels—An interpretive review. *Metall. Ital.* **2009**, *11*, 35–42. Available online: https://www.academia.edu/10782168/On_strength_of_microalloyed_steels_an_interpretive_review (accessed on 19 July 2013).
6. Larzabal, G.; Isasti, N.; Rodriguez-Ibabe, J.M.; Uranga, P. Evaluating strengthening and impact toughness mechanisms for ferritic and bainitic microstructures in Nb, Nb-Mo and Ti-Mo microalloyed steels. *Metals* **2017**, *7*, 65. [CrossRef]
7. Zaitsev, A.; Arutyunyan, N. Low-carbon Ti-Mo microalloyed hot rolled steels: Special features of the formation of the structural state and mechanical properties. *Metals* **2021**, *11*, 1584. [CrossRef]
8. Zaitsev, A.; Koldaev, A.; Arutyunyan, N.; Dunaev, S.; D'yakonov, D. Effect of the chemical composition on the structural state and mechanical properties of complex microalloyed steels of the ferritic class. *Processes* **2020**, *8*, 646. [CrossRef]
9. Sanz, L.; Pereda, B.; López, B. Effect of thermomechanical treatment and coiling temperature on the strengthening mechanisms of low carbon steels microalloyed with Nb. *Mater. Sci. Eng. A* **2017**, *685*, 377–390. [CrossRef]
10. Bu, F.Z.; Wang, X.M.; Yang, S.W.; Shang, C.J.; Misra, R.D.K. Contribution of interphase precipitation on yield strength in thermomechanically simulated Ti–Nb and Ti–Nb–Mo microalloyed steels. *Mater. Sci. Eng. A* **2014**, *620*, 22–29. [CrossRef]
11. Zhang, K.; Li, Z.; Wang, Z.; Sun, X.; Yong, Q. Precipitation behavior and mechanical properties of hot-rolled high strength Ti–Mo-bearing ferritic sheet steel: The great potential of nanometer-sized (Ti, Mo)C carbide. *J. Mater. Res.* **2016**, *31*, 1254–1263. [CrossRef]
12. Jiang, S.; Wang, H.; Wu, Y.; Liu, X.; Chen, H.; Yao, M.; Gault, B.; Ponge, D.; Raabe, D.; Hirata, A.; et al. Ultrastrong steel via minimal lattice misfit and high-density nanoprecipitation. *Nature* **2017**, *544*, 460–464. [CrossRef]
13. Kong, H.J.; Liu, C.T. A Review on nano-scale precipitation in steels. *Technologies* **2018**, *6*, 36. [CrossRef]
14. Gladman, T. Precipitation hardening in metals. *Mater. Sci. Technol.* **1999**, *15*, 30–36. [CrossRef]
15. Chen, W.; Gao, P.; Wang, S.; Lu, H.; Zhao, Z. Effect of vanadium on hydrogen embrittlement susceptibility of high-strength hot-stamped steel. *J. Iron Steel Res. Int.* **2020**, *28*, 211–222. [CrossRef]
16. Huang, W. Suppression of hydrogen-induced damage in 22MnB5 hot stamping steel by microalloying. *Mater. Chem. Phys.* **2020**, *256*, 123–129. [CrossRef]
17. Takahashi, J.; Kawakami, K.; Kobayashi, Y.; Tarui, T. The first direct observation of hydrogen trapping sites in TiC precipitation-hardening steel through atom probe tomography. *Scr. Mater.* **2010**, *63*, 261–264. [CrossRef]
18. Stopher, M.A.; Rivera-Diaz-del-Castillo, P.E.J. Hydrogen embrittlement in bearing steels. *Mater. Sci. Technol.* **2016**, *32*, 1184–1193. [CrossRef]
19. Jiao, Z.B.; Luan, J.H.; Miller, M.K.; Chung, Y.W.; Liu, C.T. Co-precipitation of nanoscale particles in steels with ultra-high strength for a new era. *Mater. Today* **2017**, *20*, 142–154. [CrossRef]
20. Rodionova, I.G.; Amezhnov, A.V.; D'yakonov, D.L.; Shaposhnikov, N.G.; Baklanova, O.N.; Gladchenkova, Y.S. Study of the effect of microstructure characteristics on corrosion resistance of cold-rolled micro-alloyed sheet steels (HSLA) of strength classes 340–420 for automobile building. *Metallurgist* **2020**, *63*, 1165–1177. [CrossRef]
21. Rodionova, I.; Amezhnov, A.; Alekseeva, E.; Gladchenkova, Y.; Vasechkina, I. Effect of carbonitride precipitates on the corrosion resistance of low-alloy steels under operating conditions of oil-field pipelines. *Metals* **2021**, *11*, 766. [CrossRef]
22. Amezhnov, A.V.; Rodionova, I.G.; Batsalev, A.I.; D'yakonov, D.L.; Shaposhnikov, N.G.; Shatskii, T.E.; Marzoeva, M.E. Effect of chemical composition and microstructure parameters on carbon and low-alloy steel corrosion resistance under oil industry pipeline operation conditions. *Metallurgist* **2019**, *62*, 1030–1038. [CrossRef]
23. Rodionova, I.G.; Amezhnov, A.V.; Kudashov, D.V.; Naumenko, V.V.; D'yakonov, D.L.; Stukalova, N.A.; Arutyunyan, N.A. Effect of heat treatment in pipe processing stage on corrosion resistance of micro-alloyed steel hot-rolled products. *Metallurgist* **2020**, *64*, 322–333. [CrossRef]
24. Rodionova, I.G.; Shapovalov, E.T.; Kovalevskaya, M.E.; Baklanova, O.N.; Burko, D.A.; Endel', N.I.; Gusev, Y.B.; Gliner, R.E.; Lamukhin, A.M.; Kuznetsov, V.V.; et al. Increasing the resistance of automobile sheet to atmospheric corrosion by optimizing its chemical composition and the parameters of the manufacturing process. *Metallurgist* **2005**, *49*, 314–323. [CrossRef]

25. Rodionova, I.G.; Amezhnov, A.V.; Shaposhnikov, N.G.; Gladchenkova, Y.S.; D'yakonov, D.L. Features of the effect of microstructure characteristics on corrosion resistance of cold-rolled high-strength low-alloy steels (HSLA) grade 260–300 for automobile building. *Metallurgist* **2020**, *63*, 920–932. [CrossRef]
26. Shaposhnikov, N.G.; Rodionova, I.A.; Pavlov, A.A. Thermodynamic development of austenite-martensite class corrosion-resistant steels intended for a bimetal cladding layer. *Metallurgist* **2016**, *59*, 1195–1200. [CrossRef]
27. Amezhnov, A.V.; Rodionova, I.G.; Kuznetsov, D.V.; Komissarov, A.A.; Sidorova, E.P. Effect of heat treatment on corrosion activity of nonmetallic inclusions and steel corrosion resistance in aqueous media. *Metallurgist* **2019**, *62*, 1232–1239. [CrossRef]
28. Townsend, H.E. Effects of alloying elements on the corrosion of steel in industrial atmospheres. *Corrosion* **2001**, *57*, 497–501. [CrossRef]
29. Nam, N.D.; Kim, M.J.; Kim, J.G. Corrosion behavior of low alloy steels containing manganese in mixed chloride sulfate solution. *Metall. Mater. Trans. A* **2014**, *45*, 893–905. [CrossRef]
30. Ralston, K.D.; Birbilis, N. Effect of grain size on corrosion: A review. *Corrosion* **2010**, *66*, 075005–075005-13. [CrossRef]
31. Ghosh, S.; Singh, A.K.; Mula, S.; Chanda, P.; Vinay, V.; Mahashabde, V.V.; Roy, T.K. Mechanical properties, formability and corrosion resistance of the mechanically controlled processed Ti-Nb stabilized IF steel. *Mater. Sci. Eng. A* **2017**, *684*, 22–36. [CrossRef]
32. Hadzima, B.; Janecek, M.; Estrin, Y.; Kim, H.S. Microstructure and corrosion properties of ultrafine-grained interstitial free steel. *Mater. Sci. Eng. A* **2007**, *462*, 243–247. [CrossRef]
33. Krishna, K.G.; Sivaprasad, K.; Sankaro Narayanan, T.S.N.; Hari Kumar, K.C. Localized corrosion of an ultrafine grained Al–4Zn–2Mg alloy produced by cryorolling. *Corros. Sci.* **2012**, *60*, 89. [CrossRef]
34. Zhang, H.; Xue, P.; Wu, L.H.; Song, Q.N.; Wang, D.; Xiao, B.L.; Ma, Z.Y. Effect of grain ultra-refinement on corrosion behavior of ultra-high strength high nitrogen stainless steel. *Corros. Sci.* **2020**, *174*, 108847. [CrossRef]